Application note

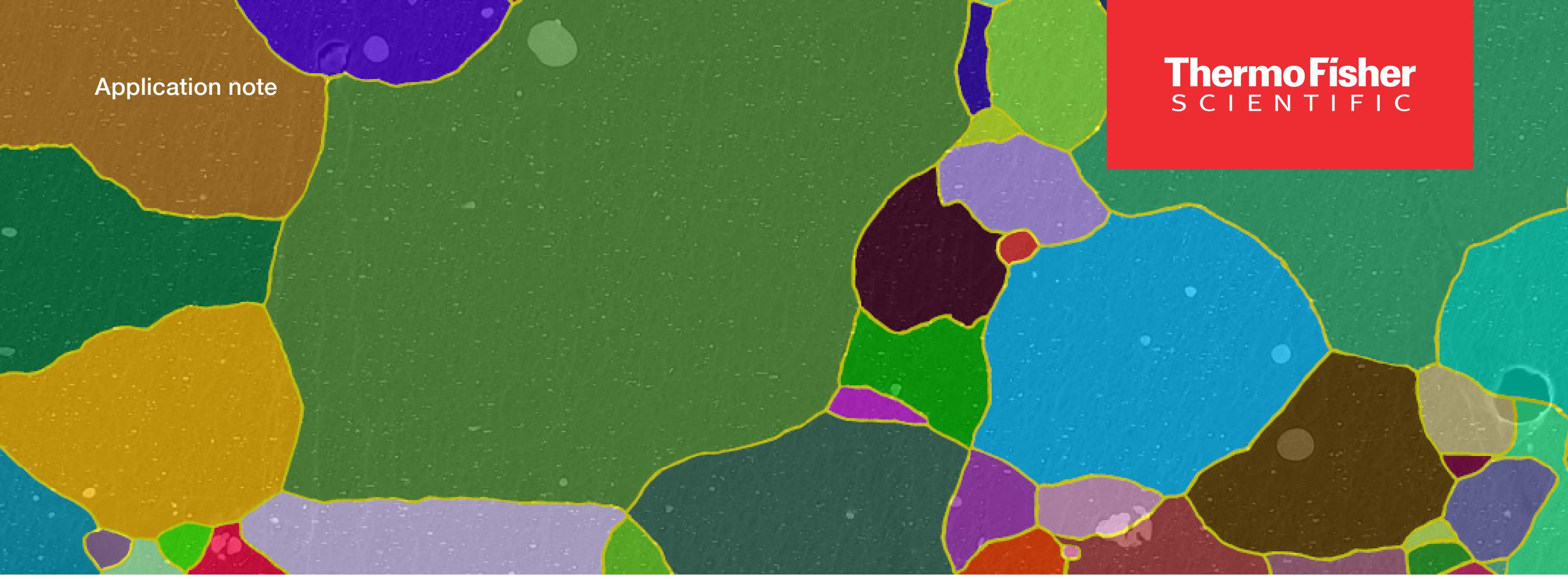

AI-assisted 2D and 3D quantification of aluminum alloy microstructure

A multimodal workflow to scale phase and grain analysis from selected micron-scale regions to large-area maps and PFIB volumes

Authors

Alice Scarpellini[1],
Hugues François-Saint-Cyr[2],
Roger Maddalena[3], Bartlomiej Winiarski[4],
Rengarajan Pelapur[2], Alexander S. Hall[2]

Introduction: from AA2024 characterization to scalable quantification

Aluminum alloys are widely used in lightweight structural applications where strength-to-weight ratio, fatigue resistance, corrosion behavior, and long-term reliability are critical. Their in-service performance and overall lifetime are strongly influenced by microstructural features such as grain structure, precipitates, and the distribution of intermetallic particles.

From a production and process-control perspective, material quality must be assessed after heat treatment to verify that the desired microstructural characteristics are achieved and remain consistent throughout manufacturing. This requires more than feature identification. Quantifying precipitates, intermetallic particles, grains, and grain-boundary features is essential for linking microstructure to mechanical behavior and corrosion response.

This application note uses AA2024-T6, a high-strength Al-Cu-Mg alloy, as a representative case study. The study showcases a multimodal SEM-based workflow that combines backscattered electron (BSE) imaging, energy dispersive X-ray spectroscopy (EDS) analysis with ChemiSEM Technology, and electron backscatter diffraction (EBSD) analysis with the Thermo Scientific™ TruePix EBSD Detector on a Thermo Scientific™ Apreo ChemiSEM™ System together with AI-assisted image analysis in Thermo Scientific™ Avizo™ 3D Pro Software 2025.1.

The objective is to move from selected region feature identification to scalable 2D and 3D quantification of grains, grain boundaries, secondary phases, and particle morphology.

1 Thermo Fisher Scientific, Eindhoven, The Netherlands
2 Thermo Fisher Scientific, USA
3 RJ Lee Group, Monroeville, Pennsylvania, USA
4 Thermo Fisher Scientific, Brno, Czech Republic

Characterization challenge: why a multimodal workflow is needed

AA2024 contains performance-relevant microstructural features across multiple length scales, including precipitates, grain-boundary phases, and constituent intermetallic particles. These secondary phases play an important role in the development of the final alloy properties and can influence corrosion behavior, fatigue response, and process quality. The T6 temper is produced by high-temperature solution treatment, quenching to room temperature to obtain a supersaturated solid solution, and artificial aging to induce controlled nanoscale precipitation.

BSE imaging provides useful contrast for visualizing particles and grain-boundaries, but it cannot reliably distinguish intermetallic particles or secondary phases with similar morphology or grayscale contrast. EDS analysis complements BSE imaging by identifying elemental distributions and supporting phase classification. Acquiring EDS-based phase information over every large-area field of view, every cross-section, or every slice in a 3D serial-section dataset can be time-consuming. For customers who need representative statistics, this creates a practical bottleneck: detailed characterization is possible but scaling that information across larger datasets requires a more efficient approach.

EBSD adds another complementary layer of information. It provides grain orientation, phase confirmation in selected regions, local misorientation, and grain-size statistics. This information helps interpret the alloy condition and relate secondary phases to the surrounding grain structure.

Manual image analysis also presents limitations. Segmenting grain boundaries, particles, and precipitates across large images or volumes is time-consuming, operator-dependent, and difficult to reproduce consistently.

An integrated multimodal workflow addresses these challenges by combining imaging, phase analysis, crystallographic information, and AI-assisted image analysis. This enables feature detection and phase classification to be extended from selected regions to larger 2D and 3D datasets.

Results: chemical and microstructural characterization

BSE imaging and EDS analysis of the sample surface revealed an abundance of secondary phases, including intermetallic particles and precipitate-related phases, distributed within the aluminum matrix and along microstructural features.

To accelerate phase identification, ChemiPhase, the phase mapping component available within ChemiSEM Technology, was used to analyze the EDS spectral data. ChemiPhase applies multivariate statistical analysis to the EDS dataset, grouping pixels with similar spectral signatures and generate composition-based phase maps. Compared with conventional interpretation of elemental EDS maps, ChemiPhase provides phase-level classification rather than only elemental distribution maps, speeding up the process of identifying and classifying the phases of interest across the selected regions.

Figure 1 shows ChemiPhase results for three secondary phase populations typically observed in AA2024-T6: S phase, shown in yellow; Al-Cu-Fe intermetallics, shown in green; and T phase, shown in pink. Understanding the distribution of S phase is particularly relevant because these precipitate-related features are linked to heat-treatment history and aging conditions and may influence intergranular corrosion behavior when present along grain boundaries. Al-Cu-Fe intermetallics, in contrast, are constituent particles associated with alloy solidification rather than aging products. From a quality-control perspective, their size, morphology, and distribution are important because coarse particles can act as local stress concentrators and potential fatigue crack initiation sites.

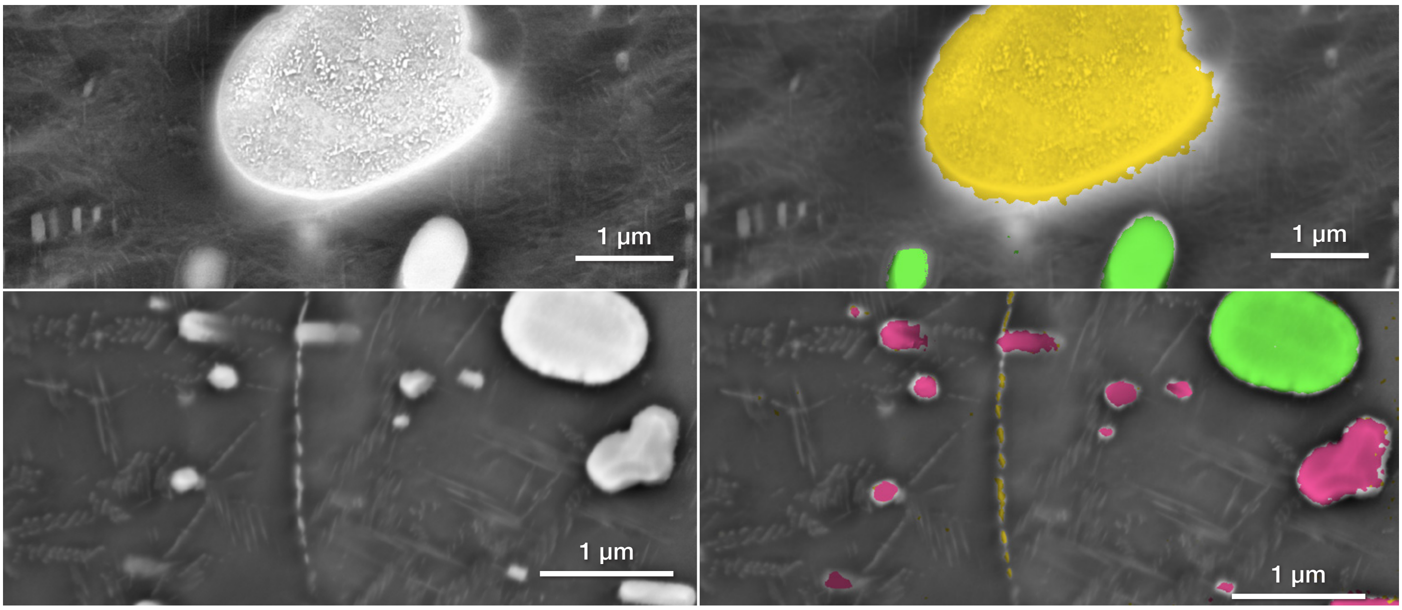

Figure 1. ChemiPhase results of three secondary phases, typically found in AA2024: S phase (yellow), Al-Cu-Fe intermetallics (green) and T phase (pink). (Acc voltage 10 kV, beam current 6.4 nA).

Following ChemiPhase phase mapping, EBSD was performed on the same region of interest shown in Figure 1. The combination of EDS analysis with ChemiSEM Technology and EBSD analysis with the TruePix detector enabled same-area chemical and crystallographic characterization.

In this high-magnification analysis, EBSD helped confirm selected secondary phases and resolve particle boundaries around fine microstructural features.

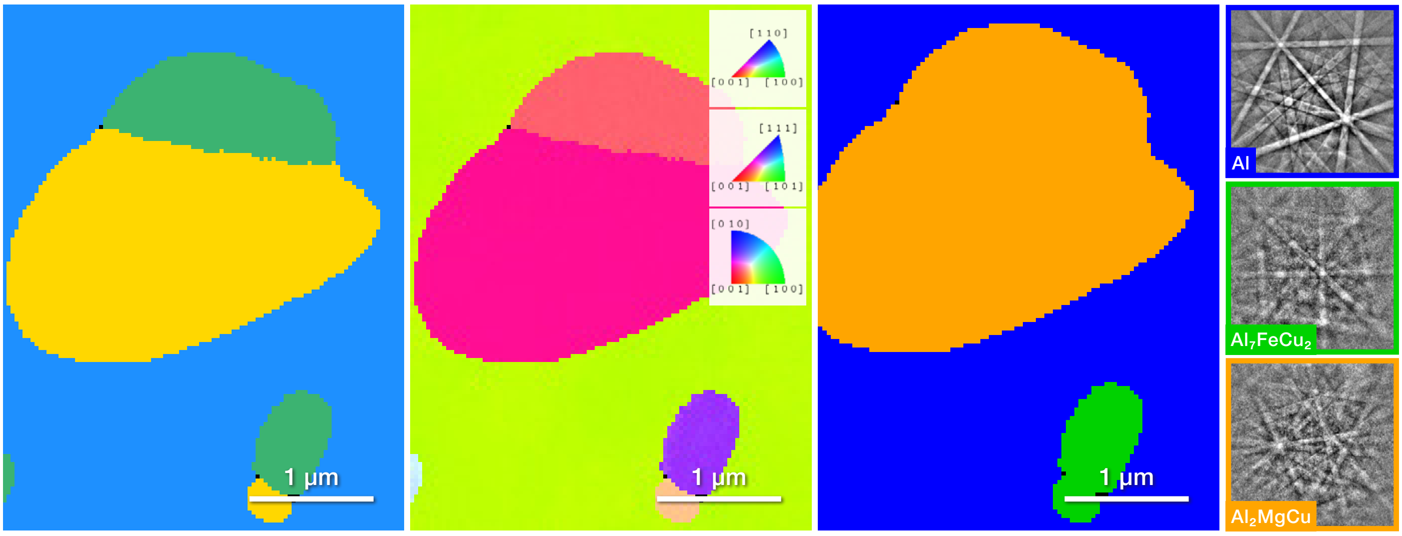

Figure 2. TruePix EBSD results of the same area of interest previously characterized with ChemiPhase (Acc voltage 10 kV, beam current 6.4 nA).

Lower-magnification EBSD characterization was then used to assess the broader grain structure of the AA2024-T6 matrix, in Figure 3.

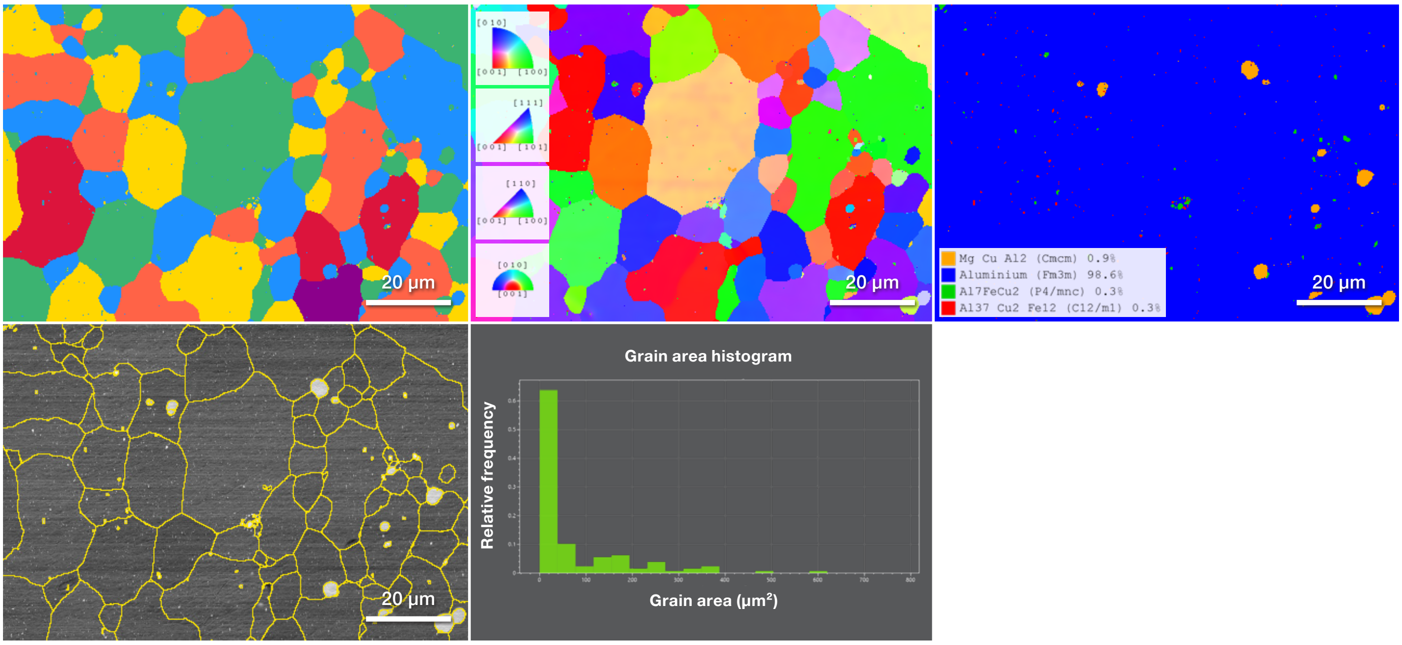

Figure 3. Base alloy characterization showing, in addition to the previous dataset, also the overlay between the grain boundaries (yellow) and the MEC image (median electron counts, an EBSD-derived intensity/contrast image created from the electron counts recorded in each EBSD pattern).

In the analyzed region, the aluminum matrix showed predominantly equiaxed grains with multiple crystallographic orientations across the field of view, consistent with a recrystallized microstructure. The broader EBSD survey revealed the presence of two Al-Cu-Fe intermetallic phase types: Al_7Cu_2Fe and $Al_{37}Cu_2Fe_{12}$. Identifying these distinct phase types provides additional insight into the intermetallic population present in the alloy.

Grain statistics provided quantitative descriptors such as grain count, mean grain area, and equivalent grain diameter. In this region, 128 matrix grains were counted after excluding intermetallic particles. The mean grain area was 74.8 μm^2, and the mean equivalent grain diameter was 6.91 µm. These measurements establish a baseline for the base alloy and can support comparison between different heat treatments, processing conditions, or alloy variants.

Results: AI model training and evaluation

While EBSD characterization provided complementary microstructural and crystallographic information, the ChemiPhase results provided the phase reference data needed for the next step of the workflow: AI model training and evaluation. To extend phase classification beyond the selected regions analyzed with ChemiPhase, a convolutional neural network was trained in Avizo Software (model based on a VGG19 U-Net deep learning architecture).

Six representative BSE image datasets, acquired from different regions of the AA2024 sample, were used for training together with their spatially registered ChemiPhase phase maps. For the main secondary phase classes, ChemiPhase provided the reference labels for S phase, T phase, and Al-Cu-Fe intermetallic particles (Figure 4). The model learned the BSE image features associated with each phase class, including grayscale contrast, particle morphology, edge contrast, local texture, and surrounding matrix context.

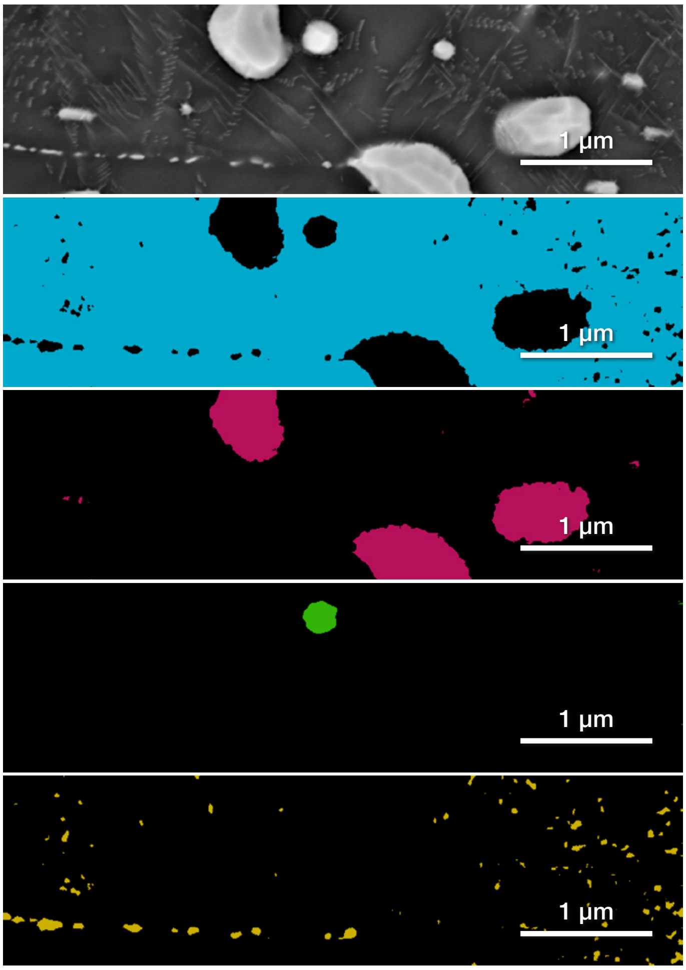

Figure 4. Example of a ChemiPhase dataset used for AI model training. Each secondary phase class is assigned a distinct color (base metal in blue, T phase in pink, Al-Cu-Fe intermetallics in green and S phase in yellow), providing the reference labels used by the model to learn phase-specific features in the corresponding BSE image.

An additional class corresponding to S' precipitates (Figure 5) was also included because these fine needle-like precipitates are key strengthening features in AA2024. Since S' precipitates are typically below the practical spatial resolution of SEM-EDS phase mapping, they were not labelled using ChemiPhase. Instead, the model was trained from image-based reference labels based on their distinctive morphology in the BSE images.

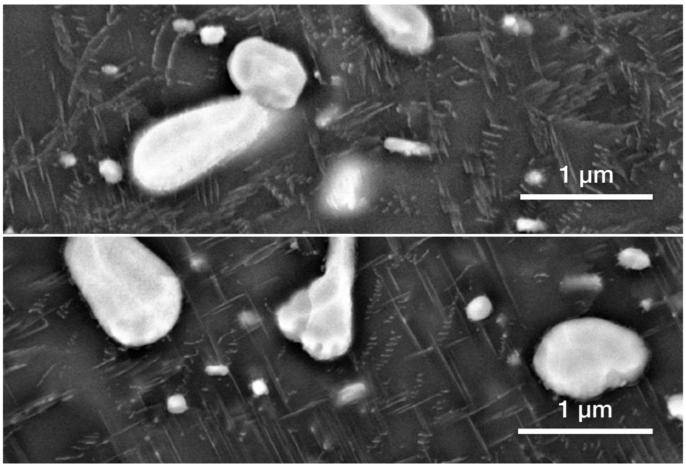

Figure 5. Examples of BSE images acquired from regions containing a high density of needle-like S' precipitate features. In these images, the visible precipitate features are typically a few hundred nanometers long, with an apparent BSE contrast width in the order of tens of nanometers.

A separate AI model was used for large-area grain-boundary identification. This model was trained to recognize the textured grain-boundary contrast visible in the BSE images and convert it into a segmentation suitable for extracting grain-boundary networks and grain-size descriptors (Figure 6).

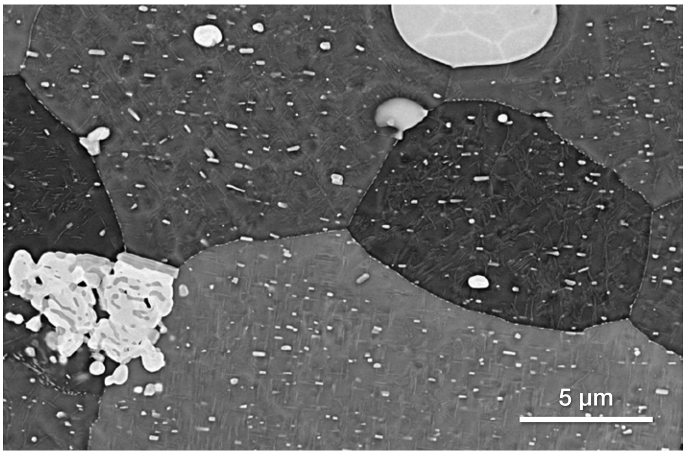

Figure 6. Example of BSE image contrast used for training the grain-boundary detection model. Grain-boundary features are visible in the image and provide the basis for AI-assisted detection over larger SEM fields of view.

Model performance was evaluated on unseen validation datasets before deployment, with the phase-classification model assessed using precision, recall, and F1 score against the corresponding reference labels (see Figure 7).

Accuracy	F1 score	Precision	Recall	Phase
98.85%	0.993	0.992	0.995	T phase
99.19%	0.889	0.891	0.888	Base metal
100%	1.00	1.00	1.00	S phase

Figure 7. Model performance evaluation results.

Together, the two AI models enabled complementary types of microstructure quantification: phase classification for secondary phases and precipitate-related features, and grain-boundary detection for matrix grain analysis. Once trained and evaluated, these models were applied to larger 2D SEM maps and 3D PFIB-SEM serial-section datasets.

Results: scaling AI-assisted analysis to 2D and 3D quantification

After training and validation, the AI models were applied to larger SEM datasets to extend the analysis beyond the selected high-magnification regions.

For 2D analysis, large-area BSE images were used as input for AI-assisted segmentation in Avizo Software. Two complementary analyses were performed. The first model was applied to identify secondary phase populations across the larger field of view, including S phase, T phase, Al-Cu-Fe intermetallic particles, and S’ precipitate-rich regions. This enabled phase-specific measurements such as area fraction, particle distribution, and spatial relationships with the surrounding matrix.

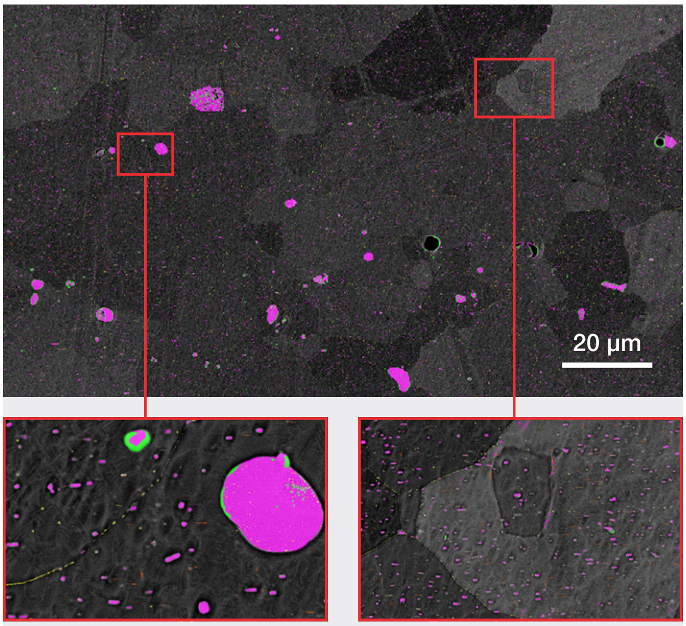

Phase	Area (nm^2)	Area fraction
T	387.23 E6	2.05%
S	3.23 E6	0.17%
IM	5.12 E6	0.27%
S’	2.56 E6	0.14%

Figure 8. Results of the phase-classification model applied to a large-area 2D BSE image. Colored overlays show the predicted distribution of T phase, S phase, Al-Cu-Fe intermetallics, and S’ precipitates. Magnified regions highlight local particle morphology and phase distribution, while the table reports phase area and area fraction extracted from the segmented image.

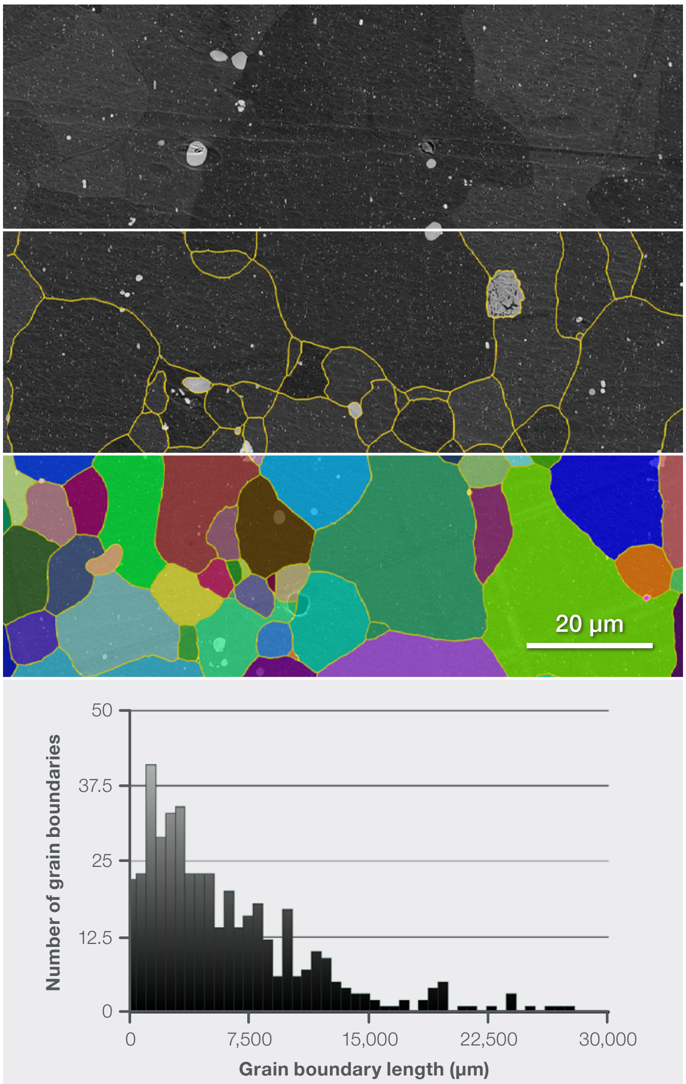

Figure 9. Results of the grain-boundary detection and grain segmentation model applied to a large-area BSE image. The workflow converts the BSE image into a detected grain-boundary network (in yellow) and individual matrix grain segmentation (multi-color overlay). A distribution of grain interface lengths is shown.

The second AI model was applied to large area BSE images acquired with Thermo Scientific™ Maps Software. The model was used to detect the grain-boundary network visible in the BSE images and, once detected, the grain-boundary information was converted into grain segmentation and spatial graph representations. This provided information on the cross-section of grain-size and grain-boundary segment length.

The trained phase-classification model (first model) was then deployed on additional datasets to evaluate scalability beyond the original selected regions. These datasets included a 3D FIB-SEM serial-section volume and automated multi-site cross sections acquired from multiple samples, including samples subjected to different heat-treatment conditions.

The 3D dataset was acquired using Auto Slice and View (ASV) Software on a Thermo Scientific™ Scios™ 3 FIB-SEM and consisted of 555 serial BSE images. The reconstructed volume was approximately 5x5x1.83 μm^3, with a slice spacing of approximately 3.3 nm. The image stack was reconstructed in Avizo Software, where the trained model was applied slice by slice to classify secondary phases throughout the volume.

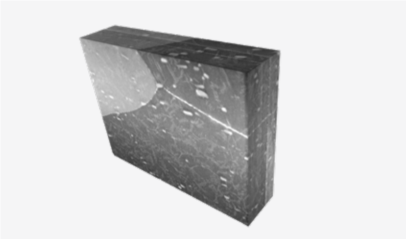

Phase	Volume (nm³)	Area fraction	Area 3D (nm²)
T	2.51 E9	0.91%	171.42 E6
IM	2.61 E9	0.95%	26.89 E6
S	0.64 E9	0.23%	46.01 E6
S'	19.73 E9	7.20%	1705.26 E6

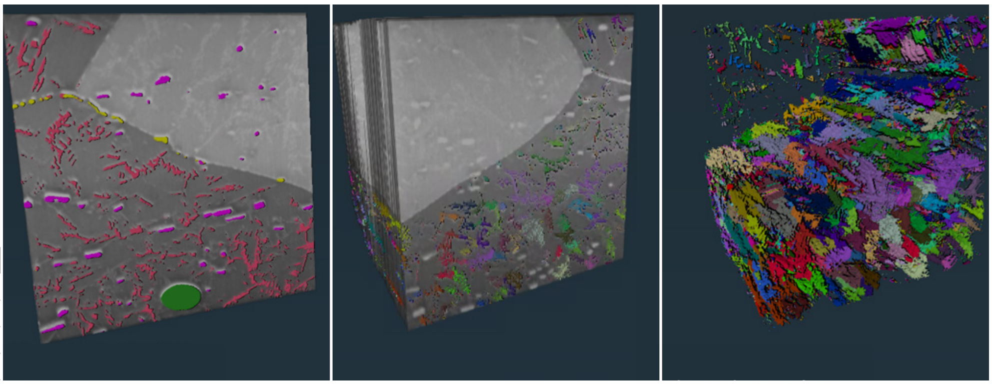

Figure 10. Results of the phase-classification model applied to a 3D BSE serial-section image stack. Colored overlays show the predicted distribution of T phase (pink); S phase (yellow); Al-Cu-Fe intermetallics (green); and S' precipitates (red). As with the 2D dataset, the table reports phase-specific metrics extracted from the segmented dataset, including phase volume, area fraction, and an estimate of 3D surface area (Area 3D). The additional view shows the S' precipitate class rendered as separated 3D objects, highlighting the ability of the model to isolate fine precipitate-rich features within the reconstructed volume.

This 3D analysis moves the workflow from area-based measurements to volume-based measurements. Instead of measuring only the apparent size and distribution of particles on a single polished surface, the reconstructed volume provides information through the depth of the material. This is particularly valuable for intermetallic particles and precipitate-related features, because their true size, shape, and connectivity may not be fully represented in a single 2D section.

To assess the applicability of the model across repeated cross-section datasets, automated cross sections were also acquired using [Auto Cross Section (AXS) software](#) on Thermo Scientific™ Scios™ 3 FIB-SEM. For each sample, nine sites were analyzed, with an acquisition time of approximately 30 minutes per site, including about 28 minutes for milling and 2 minutes for imaging. This enables the trained model to be applied across multiple regions and heat-treatment conditions, supporting more representative phase quantification.

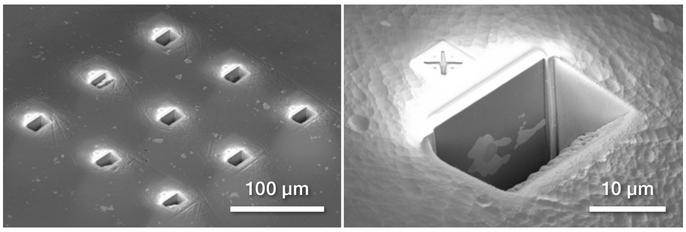

Figure 11. Automated multi-site cross-section. Multiple cross sections were milled across the sample surface using AXS automation software, enabling site-specific BSE imaging for AI-assisted phase classification across different regions or sample conditions.

Conclusions

High-performance aluminum alloys are controlled by microstructural features that are often heterogeneous and distributed across multiple length scales. Understanding these features requires statistically relevant information, especially when evaluating manufacturing processes, heat-treatment effectiveness, or process consistency. For AA2024-T6, this is particularly important because precipitates and intermetallic particles all contribute to mechanical behavior and corrosion response.

This application note demonstrates an AI-assisted workflow for scaling analysis from selected high-magnification regions to larger 2D and 3D datasets. Using AA2024-T6 as a representative case study, the workflow combines the following Thermo Scientific™ products: Apreo ChemiSEM System, TruePix EBSD Detector, Maps Software, Scios™ 3 with Auto Slice & View Software, Auto Cross Section Software, and Avizo Software.

Each part of the workflow contributes a specific type of information. Imaging and ChemiPhase phase analysis provide rapid classification of secondary phases and reference labels for AI model training, while EBSD provides complementary crystallographic and grain-structure information to support interpretation of the alloy condition and selected phase assignments. AI-assisted image analysis in Avizo Software then enables these findings to be scaled to large-area 2D datasets, 3D FIB-SEM volumes, and automated multi-site or multi-sample cross-section datasets.

The result is an integrated workflow that can provide critical insights for alloy development, heat-treatment assessment, quality control, and performance-relevant materials characterization.

Learn more at **thermofisher.com/apreo-chemisem**